THE EFFECT OF B SEGREGATION ON HEAT-AFFECTED ZONE MICROFISSURING IN EB WELDED INCONEL 718

By

M.C. Chaturvedi, W. Chen, A. Saranchuk
Department of Mechanical and Industrial Engineering
University of Manitoba, Winnipeg, Canada

And

N.L. Richards
Bristol Aerospace Ltd., Winnipeg, Manitoba

ABSTRACT

In a previous study on cast Inconel 718 it was observed that B can segregate on the grain boundaries during heat treatment and contribute to the HAZ microfissuring. In the wrought Inconel 718, however, the HAZ microfissuring has been mainly attributed to the segregation of S at the grain boundaries. Therefore, a research project was started to study the effect of B on the HAZ microfissuring of wrought Inconel 718. Two alloys with identical composition, except for the concentration of B were prepared. The alloys were given a final solution heat-treatment at 1050^{0}C to produce a single phase material. Half of the solution treated samples were water-quenched and the other half were air cooled. Although, quantitative analysis could not be performed by SIMS, qualitatively it was observed that:

(1) In the same alloy significantly more B was present at the grain boundaries of the air-cooled specimen as compared to the water-quenched specimen.

(2) The segregation of B was significantly higher in the higher B specimen as compared to the low B specimens.

The solution treated specimens were EB welded and their susceptibility to HAZ cracking was measured. It was found that the higher boron alloy specimens were more susceptibility to cracking. Also the material that was air cooled from this solution treatment temperature was more susceptible to HAZ cracking as compared to the water-quenched specimen.

Superalloys 718, 625, 706 and Various Derivatives
Edited by E.A. Loria
The Minerals, Metals & Materials Society, 1997

INTRODUCTION

The incidence of heat affected zone (HAZ) cracking around welded joints in Inconel 718 has been extensively studied[1-15], although wrought alloys have received more attention than the cast alloys. It is widely accepted that constitutional liquation of NbC and Laves phases, and of borides[16] and silicides[12] to a smaller extent, during the heating cycle associated with the welding process to be the primary cause of HAZ cracking. The formation of liquid film at the grain boundaries, where most of these particles are located, reduce the ability of the grain boundaries to support welding stresses which leads to the formation of cracks in the HAZ. However, recently the segregation of solute atoms and impurity or tramp elements has been also suggested to be responsible for HAZ cracking. The segregation of impurities can take place during heat treatment of the material prior to welding by both equilibrium and non-equilibrium segregation mechanisms. Segregation of some elements can reduce the melting point of the grain boundary material relative to the surrounding matrix. The segregated grain boundaries have the potential of liquating during the welding process giving rise to HAZ cracking in welded joints. The influence of segregation of sulfur at grain boundaries in HAZ cracking of welded Inconel 718 has been extensively studied by the research group of Thompson by using Auger spectroscopy. However, Huang, Chaturvedi and Richards used Secondary Ion Mass spectroscopy to study the effect of prior heat treatment on the equilibrium and non-equilibrium segregation of B at the grain boundaries of cast Inconel 718. They concluded that B also plays a significant role in causing HAZ microcracking in electron beam welded cast Inconel 718[17]. To confirm the role of B segregation on HAZ microcracking, special alloys based on Inconel 718 were made with controlled amount of B and very low amounts of S, C and P. The preweld heat treatments were designed to eliminate the presence of Laves phases, carbides and borides in the microstructure, and produce different levels of segregation of B at the grain boundaries. In this communication, results of the investigation carried out so far are being presented.

EXPERIMENTAL

Two Inconel based alloys whose chemical composition were identical except for boron, which was 43 and 11 ppm respectively, with the lowest possible carbon, sulfur and phosphorus were used in the study. Fifteen pound melts of these alloys were made by Special Metals Corporation using standard commercial VIM practice and hot rolled to 12.5 mm thick plates. The chemical composition of the alloys is given in Table I. The as-received material was homogenized at 1200°C in a furnace with flowing argon and then quenched in water. Through a series of cold rolling and annealing treatments at 1030°C, 6 mm thick specimens with a grain size of 100 μm were produced. The specimens were water quenched from the annealing temperature. Two specimens of each of the two alloys were then annealed at 1050°C. One of the two samples was air cooled and another was water-quenched. The microstructures of all the four samples were examined optically and by JEOL-840 SEM equipped with TN 5500 EDS System. The segregation of boron was studied by using a Cameca IMS 4f magnetic sector dynamic SIMS. An O_2^+ primary

ion beam with detection of negative secondary ions was used to investigate the distribution of B in the samples.

Table I: Chemical Composition of the Experimental Inconel 718 (wt%)

Alloy	Ni	Cr	Nb	Mo	Ti	Al	Si	Mn	Co	Ta	Zn
A	52.5	19.0	5.0	3.0	1.0	0.5	<0.2	<0.35	<0.1	<0.1	<0.03
B	52.5	19.0	5.0	3.0	1.0	0.5	<0.2	<0.35	<0.1	<0.1	<0.03

Alloy	S	P	C	B	Fe
A	0.0009	0.007	0.002	0.0043	Bal
B	0.0008	0.0066	0.003	0.0011	Bal

The heat treated samples were electron beam welded by using bead-on-plate technique at a speed of 150 cm/min, a voltage of 44 Kv and a current of 79mA. The welded samples were sectioned, polished and lightly etched and their HAZ cracking behavior was examined by measuring total crack length, total number of cracks and average crack length in an SEM.

RESULTS AND DISCUSSION

Preweld Heat Treatments

The preweld heat-treatments influence the grain size, presence of second phases and segregation, both equilibrium and non-equilibrium, which in turn influences the HAZ cracking of a material. The solution heat-treatment temperatures were kept above the Laves phase solvus temperature to produce a single phase material. A very carefully designed thermo-mechanical treatment scheme was used to maintain the same grain size in all the four specimens of both the high and low B materials. The solution heat-treatment time was determined by the expression $t \propto d^2/D$, where $D = 2 \times 10^{-7} \exp(-0.91\ eV/KT)\ m^2/s$ is the diffusion coefficient of boron, d is the diffusion distance which was set to be equal to 4 times the grain size in order to achieve the same level of equilibrium segregation of boron in all the samples. The grain size of the specimens was $100 \pm 6.0\ \mu m$. The final solution heat-treatment time was calculated to be 9.6 min at 1050°C to attain an equilibrium segregation of B. After this treatment two samples were air cooled at a cooling rate of 117°C/sec and another two samples were water-quenched which produced a cooling rate of 570°C/sec. The grain size of the specimens after this heat-treatment remains unchanged at about 100 μm. The microstructure of all the four samples was single phase without the presence of Laves phase. However, a few undissolved particles were occasionally observed at the grain boundaries. An example is shown in Fig. 1 which is the SEM micrograph of a high boron alloy solution treated and water-quenched.

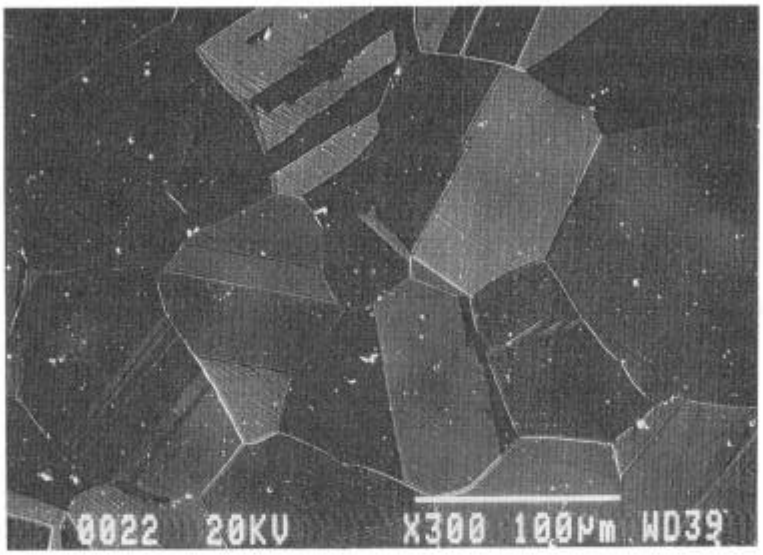

Figure 1: SEM micrograph of the high B specimen water-quenched from 1050°C.

Grain Boundary Segregation of Boron

The optimum way to detect boron in SIMS is as the molecular secondary ion $^{10}B^{16}O_2$ which has a mass of 42 as compared to the secondary ion $^{11}B^+$. The use of weaker ^{10}B isotope avoids the potential mass interference at mass 43 ($^{11}B^{16}O^-_2$) with $^{27}Al^{16}O$. Direct images of the selected ions of elements and molecules were acquired by operating SIMS in the ion microscope mode, while retaining sufficient mass resolution to eliminate potential mass interference. This involved the illumination of the sample by a primary beam of 50-100 µm diameter which generated secondary ions from all the parts illuminated by the beam in a planar electrostatic field. The lateral distribution of these secondary ions was retained through the mass spectrometer system. After energy and mass filtering the resulting images were recorded on a restive anode encoder which localized the ion signals in the image plane of the detector and recorded the ion intensity in the image. An acquisition time of 90-150 seconds was used and on the average about 20 areas of each of the four specimens were examined. It was found that in the high boron alloy many more grain boundaries had boron segregated on them as compared to the low boron alloy. Although a quantitative analysis of boron segregation could not be performed, however, qualitatively the intensity of boron segregation was observed to be significantly higher in the air-cooled specimen as compared to the water-quenched specimen. An example is shown in Fig. 2 a.b., which are the boron ion images of the high boron alloy specimens air-cooled and water-quenched, respectively, from 1050°C solution treatment temperature. The segregation of boron is visible in the air-cooled (Fig. 2a) specimens whereas in the water-quenched specimen (Fig. 2b) the grain boundaries are almost clean. A similar trend was also observed in specimens that were solution treated at 1100, 1150 and 1200°C. The least amount of boron segregation on grain boundaries was observed in the low boron specimen that was water-quenched from the solution treatment temperature.

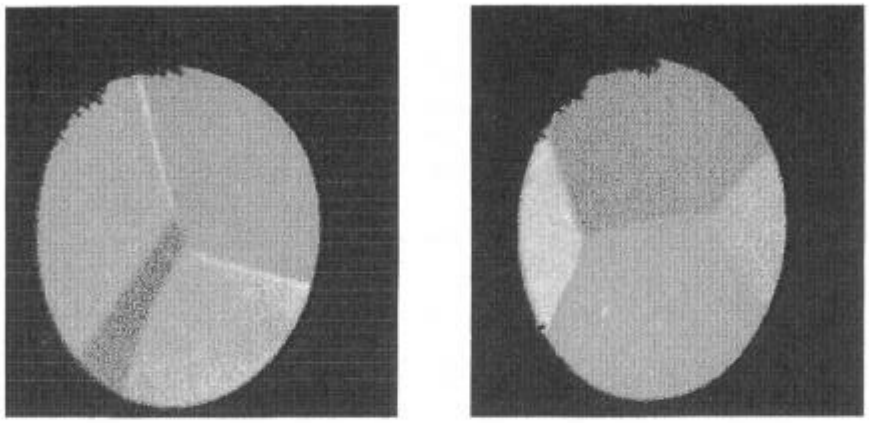

a b

Figure 2: SIMS B ion images of the high B material. (a) Air-cooled (117°C/s). Two white GB reflect B segregation. (b) Water-quenched (570°C/s) B segregation on GB is not observed.

Susceptibility To HAZ Cracking

The heat-treated samples were electron beam welded using the parameters described in Section 2. The electron beam welding produced a nail-shape fusion zone as illustrated in Fig. 3.

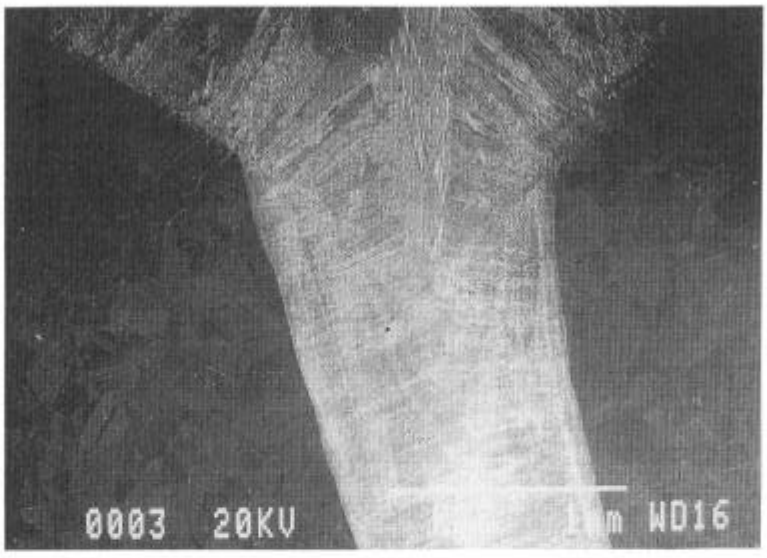

Figure 3: SEM micrograph of an EB weld.

Intergranular cracks were observed in the HAZ around fusion zone, an example of which is shown in Fig. 4. It was also noted that more cracks were present in the nail shoulder region as compared to the other locations in the HAZ. In the low boron material very few cracks were seen even in the shoulder region. The cracking susceptibility of all the four samples was quantitatively assessed by SEM. For this, the welded pieces were cut in a direction perpendicular to the welding direction, polished and lightly etched. A total of eight such metallographic specimens were examined for each of the four welded samples. The total number of cracks, total crack length and average crack length were measured. The values of these parameters for the four specimens is given in Table II. It is seen that for a given alloy the total crack length was larger in air cooled material and the number of cracks were also larger. The average crack length, however, was almost the same. For a given solution heat-treatment temperature, higher boron content alloy was more susceptible to cracking than the low boron alloy.

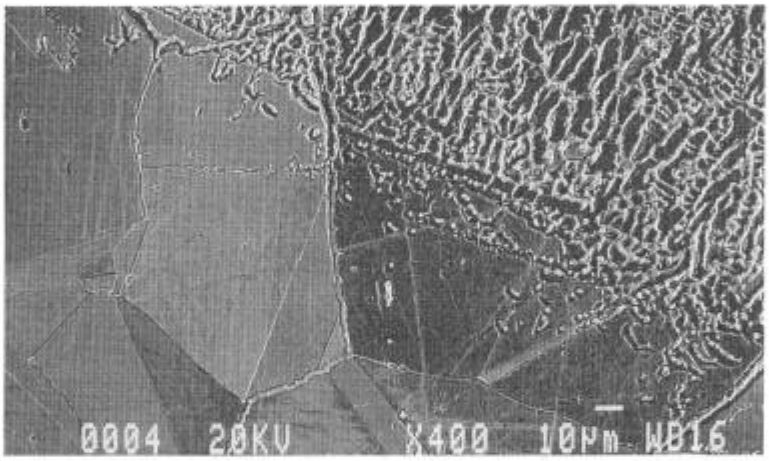

Figure 4: SEM micrograph of HAZ around EB weld in the high boron material showing cracks at GB.

Table II: Cracking Parameters

Alloy	Total Crack Length* µm	No. of Cracks	Average Crack Length* µm
High B Alloy Air Cooled	3134 ± 925	33	96.6 ± 21.4
High B Alloy Water-Quenched	1770 ± 433	24	75.9 ± 27.1
Low B Alloy Air Cooled	2348 ± 129	7	32.8 ± 13.7
Low B Alloy Water-Quenched	1517 ± 83.6	5	31.8 ± 21.9

** 90% confidence limit*

Grain Boundary Segregation of B and Susceptibility to HAZ Cracking

In a previous study in Cast Inconel 718 it was suggested that the segregation of B to the grain boundaries was non-equilibrium type[17]. Subsequently, our studies on experimental wrought Inconel 718 based alloys using SIMS analysis further confirmed this observation[18]. The non-equilibrium segregation can occur during cooling from the solution heat-treatment temperature due to the tendency of the vacancy-boron complexes to diffuse to the grain boundaries and get annihilated. The extent of this type of segregation will depend upon the solution heat-treatment temperature, concentration of boron and the cooling rate. A very fast cooling rate will allow a very short time for the solute-vacancy complex to diffuse to the grain boundary. Whereas, a very slow cooling may cause back flow of the segregated solute atoms to the interior of the grains due to the concentration gradient between the grain boundaries and the grain interior. Although, quantitative analysis could not be carried out by SIMS, qualitatively it was observed that the intensity of boron images was higher in high boron material. It was also higher in the material that was air cooled at 170°C/s as compared to the water-quenched material.

The segregation of boron to grain boundaries correlates extremely well with the HAZ cracking susceptibility of the material. That is, the higher boron containing material has significantly greater cracking susceptibility as compared to the low boron containing material, regardless of the cooling rate from the solution treatment temperature (Table II).

Furthermore, air cooled material, where the segregation of boron was larger than that observed in the water-quenched material, was more susceptible to HAZ cracking than the water-quenched material.

As stated earlier, in a commercial Inconel 718 HAZ cracking has been generally attributed to the constitutional liquation. Thompson et al[10] have suggested that during the heating cycle of the welding process, Nb rich carbides and/or Laves phases liquate and start feeding Nb to the surrounding matrix by high temperature diffusion. When Nb in the surrounding area reaches about 50 wt% eutectic melting occurs. As temperature continues to rise, melting of Nb rich matrix continues and liquid spreads along the grain boundaries. After the welding, during cooling, strain builds up around the liquid at the grain boundaries and microfissures are formed. At the same time resolidification of the matrix and Laves phase occur at the liquated grain boundaries. Therefore, one of the characteristic features of the cracking in the HAZ is due to constitutional liquation is the presence of resolidified products around the cracks. In the alloys used in this study, Laves phases prone to constitutional liquidation were almost absent. However, many cracks were seen to be associated with resolidified products around them. An example shown in Fig. 5. Therefore, it seems that the cracks in the material also formed by the same mechanisms as that proposed for that material which contain liquation susceptible phases. It has been suggested that boron can lower the melting point of grain boundaries and also decrease their weldability[18,19]. Recently

it has been reported that the addition of 70 ppm B in Inconel 718 can lower its melting point by 70°C[20].

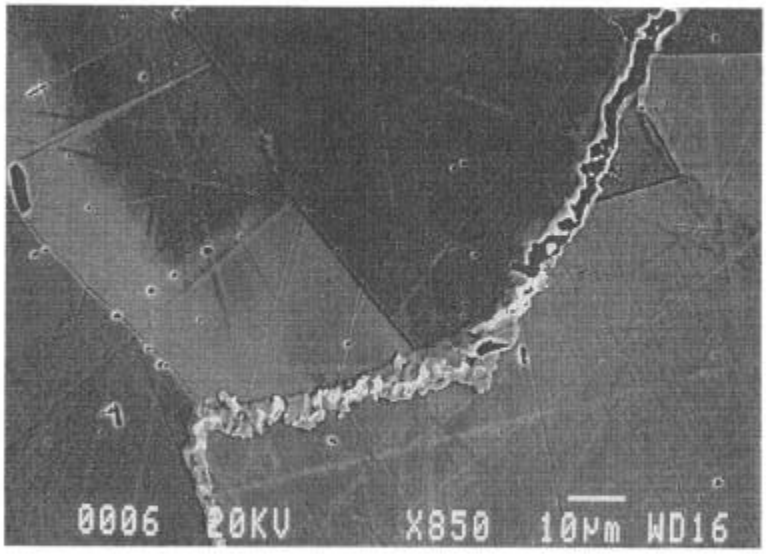

Figure 5: SEM micrograph of GB in HAZ of an air cooled high B material.

Therefore, it is suggested that in the alloys used in this study segregation of boron liquated the grain boundaries during the heating cycle which led to the formation of cracks and the susceptibility of the material to HAZ cracking is related to the degree of boron segregation, which in turn is related to the overall boron concentration and the pre-weld heat treatment, especially the cooling rate from the solution heat-treatment temperature.

CONCLUSIONS

1. Boron segregated to the grain boundaries of boron containing Inconel based superalloys, which were almost free of S, P and C, during the preweld solution heat-treatment conducted at 1050°C. The solution treated microstructure was single phase and almost free of any second phase particles.
2. Qualitatively it was observed that the grain boundary segregation of boron was larger in higher boron material as compared to the low boron material. B segregation was also higher in the specimen of the same alloy which was air cooled (117°C/s) as compared to the specimen that was water-quenched (570°C/s) from the solution heat-treatment temperature.
3. The HAZ cracking susceptibility was higher for the alloy that contained more boron as compared to the lower boron alloy. It was also higher for the air cooled as compared to the water-quenched specimen of the same alloy. It is therefore, suggested that since the segregation of boron can lower the melting point of the grain boundary material, HAZ cracking in this alloy is caused by the segregation of boron to the grain boundaries.

ACKNOWLEDGMENTS

The authors would like to thank the consortium of Manitoba aerospace industries and the Natural Sciences and Engineering Research Council of Canada for their financial support, and to Dr. G. McMahon and Dr. T. Malis of Materials Technology Laboratory of Natural Resource Canada, Ottawa, for facilitating SIMS analysis. Thanks are also due to Special Metals Corporation for making the alloys.

REFERENCES

1. X. Huang, N.L. Richards and M.C. Chaturvedi, Metall. Trans., 27A (1996), 785.
2. B. Radhakrishnan and R.G. Thompson, Metall. Trans., 24A (1993) 1409.
3. B. Radhakrishnan and R.G. Thompson, Metall. Trans., 23A (1992) 1783.
4. R.G. Thompson, D.E. Mayo and B. Radhakrishnan, Metall., 22A (1991) 557.
5. B. Radhakrishnan and R.G. Thompson, Metall. Trans., 22A (1991) 887.
6. B. Radhakrishnan and R.G. Thompson, Metall. Trans., 20A (1989) 2866.
7. R.G. Thompson, J. Met., July (1988) 44.
8. T.J. Kelly, in "Advances in Welding Science and Technology", S.A. David, Eds. 1986, p. 623.
9. R.G. Thompson, J.R. Dobbs, and D.E., Mayo, Weld J., 65 (11) (1986) 299s.
10. R.G. Thompson, J.J. Cassimus, D.E. Mayo and J.R. Dobbs, Weld J., 64 (4) (1985) 91s.
11. R.G. Thompson and S. Genculu, Weld, J., 62 (12) (1983) 337s.
12. E.G. Thompson, Weld, J., 48 (2) (1969) 70s.
13. D.S. Duvall and W.A. Owczarski, Weld, J., 46 (1967) 423s.
14. W.A. Owczarski, D.S. Duvall and C.P. Sullivan, Weld, J., 45 (1966) 145s.
15. A.D. Romig, Jr., J.C. Lippold and M.J. Cieslak, Metall. Trans., 19A (1988) 35.
16. R. Vincent, Acta Metall., 33 (7) (1985) 1205.
17. X. Huang, M.C. Chaturvedi, N.L. Richards and J. Jackman: Acta Materialia (in Press).
18. W. Chen, M.C. Chaturvedi, N.L. Richards and C. McMahon: To be published.
19. Hugh Baker, ASM Handbook, Vol. 3, Alloy Phase Diagrams, The Materials Information Society, 1992, p. 2.83.
20. Y. Zhu, S. Zhang, T. Zhang, L. Lou, Y. Tong, X. Ning, Z. Hu and X. Xie, in Superalloys 718, 625, 706 and Various Derivatives, Ed. E.A. Loria, The Minerals, Metals and Materials Society, 1994, p. 89.